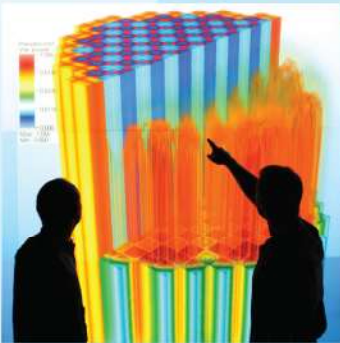


DISCLAIMER

This report was prepared as an account of work sponsored by an agency of the United States Government. Neither the United States Government nor any agency thereof, nor any of their employees, makes any warranty, express or implied, or assumes any legal liability or responsibility for the accuracy, completeness, or usefulness of any information, apparatus, product, or process disclosed, or represents that its use would not infringe privately owned rights. Reference herein to any specific commercial product, process, or service by trade name, trademark, manufacturer, or otherwise does not necessarily constitute or imply its endorsement, recommendation, or favoring by the United States Government or any agency thereof. The views and opinions of authors expressed herein do not necessarily state or reflect those of the United States Government or any agency thereof. Reference herein to any social initiative (including but not limited to Diversity, Equity, and Inclusion (DEI); Community Benefits Plans (CBP); Justice 40; etc.) is made by the Author independent of any current requirement by the United States Government and does not constitute or imply endorsement, recommendation, or support by the United States Government or any agency thereof.



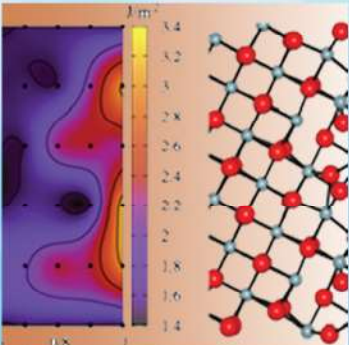
Power uprates
and plant life extension



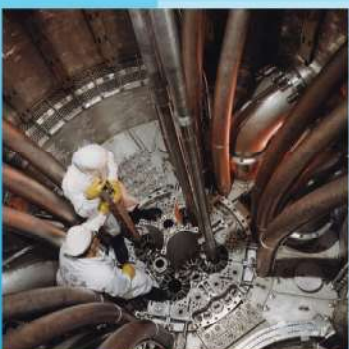
Engineering design
and analysis



Science-enabling
high performance
computing



Fundamental science



Plant operational data



L3:RTM.PRT.P9.02 Demonstration of Full Core Reactor Depletion with MPACT

Revision 0

Benjamin Collins
Aaron Graham
Ang Zhu
Brendan Kochunas
Tom Downar

Radiation Transport Methods
Oak Ridge National Laboratory

August 10, 2014



U.S. DEPARTMENT OF
ENERGY

Nuclear Energy

DOCUMENT AVAILABILITY

Reports produced after January 1, 1996, are generally available free via US Department of Energy (DOE) SciTech Connect.

Website www.osti.gov

Reports produced before January 1, 1996, may be purchased by members of the public from the following source:

National Technical Information Service
5285 Port Royal Road
Springfield, VA 22161
Telephone 703-605-6000 (1-800-553-6847)
TDD 703-487-4639
Fax 703-605-6900
E-mail info@ntis.gov
Website <http://classic.ntis.gov/>

Reports are available to DOE employees, DOE contractors, Energy Technology Data Exchange representatives, and International Nuclear Information System representatives from the following source:

Office of Scientific and Technical Information
PO Box 62
Oak Ridge, TN 37831
Telephone 865-576-8401
Fax 865-576-5728
E-mail reports@osti.gov
Website <http://www.osti.gov/contact.html>

This report was prepared as an account of work sponsored by an agency of the United States Government. Neither the United States Government nor any agency thereof, nor any of their employees, makes any warranty, express or implied, or assumes any legal liability or responsibility for the accuracy, completeness, or usefulness of any information, apparatus, product, or process disclosed, or represents that its use would not infringe privately owned rights. Reference herein to any specific commercial product, process, or service by trade name, trademark, manufacturer, or otherwise, does not necessarily constitute or imply its endorsement, recommendation, or favoring by the United States Government or any agency thereof. The views and opinions of authors expressed herein do not necessarily state or reflect those of the United States Government or any agency thereof.

REVISION LOG

Revision	Date	Affected Pages	Revision Description
0	8/10/2014	All	Original Report

Document pages that are:Export Controlled NoneIP/Proprietary/NDA Controlled NoneSensitive Controlled None**Requested Distribution:**

To: N/A

Copy:N/A

Contents

1.0 Introduction	1
2.0 Depletion Methodology	2
3.0 Boron 10 Depletion Methodology	9
4.0 Simplified Thermal Hydraulic Feedback	9
5.0 Simulation of Watts Bar Cycle 1 Depletion	10
6.0 Summary and Future Work	13
References	14

1.0 Introduction

MPACT is a three-dimensional (3-D) whole core transport code capable of generating sub-pin level power distributions. This feature is accomplished by obtaining the integral transport solutions to the heterogeneous reactor problem in which the actual detailed geometrical configuration of fuel components such as the pellet and cladding is modelled explicitly. The cross section data needed for the neutron transport calculation are obtained directly from a multigroup microscopic cross section library similar to those used in lattice physics codes. Hence MPACT involves neither *a priori* homogenization nor group condensation for the core spatial solution.

The integral transport solution is obtained by means of the method of characteristics (MOC) that employs discrete ray tracing. Since the direct application of the 3-D MOC capability in MPACT to 3-D core configuration requires considerable amounts of memory and computing time for practical reactor applications, an alternative approximate 3-D solution method was implemented in MPACT based on a 2D-1D approach which employs planar MOC solutions in the framework of the 3-D coarse mesh finite difference (CMFD) formulation. The axial coupling is resolved by one-dimensional (1-D) diffusion solutions and the planar and axial problems are coupled through the transverse leakage. The use of a lower order 1-D solution in the axial direction is justified by the fact that most heterogeneity in the core occurs in the radial direction rather than the axial. However, it is possible to use one of the higher order methods in MPACT such as the 1-D SN kernel if improved solution accuracy is desired.

The CMFD formulation which originally served as an efficient nodal formulation is used in MPACT to accelerate the whole core transport calculation. The basic mesh in the CMFD formulation is a pin cell which is much coarser than the flat source regions defined for MOC calculations. The concept of dynamic homogenization of group constants for the pin cells provides the basis of the CMFD formulation in whole core transport calculation. The intra-cell flux distribution determined from the MOC calculation is used to generate the homogenized cell constants while the MOC cell surface averaged currents are used to determine the radial nodal coupling coefficients. This dynamic implementation of the equivalence theory formulation ensures the same transport solution is obtained with CMFD as the one obtained using unaccelerated MOC calculations alone.

The ability of MPACT to predict the Hot, Zero Power (HZP) condition of a reactor was reported in CASL-U-2014-0045-000. The purpose of this report is to demonstrate the capability of MPACT to simulate the operation of a reactor at Hot, Full Power (HFP) conditions during normal operation throughout a full operating cycle. The time scale for a reactor burnup cycle is typically one to two years and therefore short time phenomena such as the effect of delayed neutrons can be neglected. Instead the time dependence can be treated quasi-statically using the depletion algorithm presented in CASL-U-2013-0276-001. The full power operation requires thermal hydraulic feedback to be present during the entire simulation which will utilize the work in CASL-U-2014-0051-000. However, due to the significant computational burden of the coupled physics simulation, a simplified thermal hydraulic model is used for the analysis reported here which is principally intended to demonstrate the full core neutronics depletion. In addition to the thermal hydraulic feedback, the effect of Boron 10 depletion should be modeled in cases where major boron additions are not performed for extended periods of time. Each of these capabilities will be described in the following sections.

2.0 Depletion Methodology

A general expression for the depletion of a nuclide by a neutron reaction or radioactive decay can be written as follows:

$$\frac{dX_i(t)}{dt} = \sum_{j=1}^N \ell_{ij} \lambda_j X_j + \bar{\phi} \sum_{k=1}^N f_{ik} \sigma_k X_k - (\lambda_i + \sigma_i \bar{\phi}) X_i \quad (i = 1, \dots, N) \quad \text{Eq. (1)}$$

where

$X_i(t)$	particle density of nuclide i
λ_i	the radioactive disintegration constant for nuclide i
σ_i	the 1-group neutron absorption cross section of nuclide i
$\bar{\phi}$	the 1-group neutron scalar flux
ℓ_{ij}	the fractions of radioactive disintegrations by nuclide j which lead to the formation of nuclide i
f_{ik}	the fractions of neutron reactions by nuclide k which lead to the formation of nuclide i .

If the nuclide concentrations of several species are expressed as a vector $\vec{X} = (X_1, \dots, X_i, \dots, X_N)^T$, then the rate of change of the material composition for a homogenous region can then be expressed as a homogenous system of coupled linear first order ordinary differential equation as follows:

$$\frac{d\vec{X}}{dt} = \mathbf{A} \cdot \vec{X} \quad \text{Eq. (2)}$$

where \mathbf{A} is a $N \times N$ matrix constructed from characteristic neutron reaction rates and fractions and radioactive decay rates and fractions. The matrix exponential method can then be applied to obtain the solution of Eq. (2) as follows:

$$\vec{X}(t) = \exp(\mathbf{A}t) \cdot \vec{X}(0) \quad \text{Eq. (3)}$$

where a vector $\vec{X}(0)$ represents the known particle number densities at the beginning of the time step. Obtaining $\vec{X}(t)$ then becomes a matter of calculating $\exp(\mathbf{A}t)$, which can be done through a Taylor series expansion of the matrix exponential.

$$\exp(\mathbf{A}t) = I + \mathbf{A}t + \frac{(\mathbf{A}t)^2}{2!} + \dots = \sum_{m=0}^{\infty} \frac{(\mathbf{A}t)^m}{m!} \quad \text{Eq. (4)}$$

If all the nuclides are included in the transition matrix, then \mathbf{A} becomes a very large sparse and ill-conditioned matrix that complicates the solution of the matrix exponential equation Eq. (3). Issues can also arise in obtaining sufficient accuracy of the solution using the matrix exponential method because of the floating point arithmetic involved in the summation of very large and very small

numbers.

Since the full transition matrix cannot be solved efficiently by the matrix exponential method, the matrix is divided into two parts; one for long-lived nuclides and the other for short-lived nuclides. Then the matrix exponential in Eq. (2) can be accurately computed for just the long-lived nuclides. The criterion for the matrix separation is based on the “removal” half-life of a nuclide where the long-lived nuclides are defined such that the irradiation time interval is less than 10 times their removal half-life, since any concentration of a nuclide essentially becomes zero after 10 half-lives.

$$\Delta t \leq 10t_{r,1/2}$$

$$\text{where } t_{r,1/2} = \frac{\ln 2}{\lambda_i + \sigma_i \bar{\phi}} \quad \text{Eq. (5)}$$

To insure that the error of truncating the series expansion to a finite number of terms does not yield incorrect results, the number of terms used is determined dynamically based on the matrix norm defined by Eq. (6).

$$[\mathbf{A}] = \min \left(\max \left(\sum_{i=1}^N |a_{ij}| \right), \max \left(\sum_{j=1}^N |a_{ij}| \right) \right) \quad \text{Eq. (6)}$$

The nuclide number densities for short-lived nuclide chains beginning with a long-lived precursor are calculated using an iterative method. The short-lived daughter is assumed to be in secular equilibrium with its parent at the end of any time interval. The concentration of the parent is obtained from the exponential matrix method and the concentration of the daughter is calculated assuming its time rate of change is zero.

$$\dot{X}_i = 0 = \sum_{j=1}^N a_{ij} X_j \quad \text{Eq. (7)}$$

Eq. (7) can be solved easily using a Gauss-Seidel iteration. The coefficients in Eq. (7) have the property that all the diagonal elements of the matrix are negative and all off-diagonal elements are positive. The algorithm involves inverting Eq. (7) and using assumed or previously calculated values for the unknown concentrations to estimate the concentration for the next iteration:

$$X_i^{k+1} = -\frac{1}{a_{ii}} \sum_{\substack{j=1 \\ j \neq i}}^N a_{ij} X_j^k \quad \text{Eq. (8)}$$

The iterative procedure has been found to converge very rapidly since, for these short-lived isotopes, cyclic chains are not usually encountered and the procedure reduces to a direct solution.

For the full depletion chain, only the non-zero elements of the transition matrix are stored in two MPACT arrays for the diagonal and off diagonal elements. These coefficients are based on those

found in Eq. (1) when it is written explicitly for each nuclide X_i . However, since only long-lived nuclides are considered in the matrix exponential method, a reduced transition matrix needs to be formulated.

A generalized treatment of the full transition matrix to produce the reduced transition matrix is achieved by searching through the decay chain and forming a queue of all short-lived precursors for an isotope. The queue is terminated when the farthest removed precursor is no longer short-lived. The solution of the Bateman equation is then applied to this queue to obtain the rate constants for the reduced transition matrix. For an arbitrary forward branching chain the general solution for the i^{th} member in a chain at time t may be written in the form:

$$X_i(t) = X_i(0)e^{-d_i t} + \sum_{k=1}^{i-1} X_k(0) \left[\sum_{j=k}^{i-1} \frac{e^{(-d_j t)} - e^{(-d_i t)}}{(d_i - d_j)} a_{j+1,j} \prod_{\substack{n=k \\ n \neq j}}^{i-1} \frac{a_{n+1,n}}{d_n - d_j} \right] \quad \text{Eq.(9)}$$

The notation $a_{i,j}$ for the first-order rate constant is the same as described before, and $d_i = -a_{i,i}$. In the present application, Eq.(9) is recast in the form

$$X_i(t) = X_i(0)e^{-d_i t} + \sum_{k=1}^{i-1} X_k(0) \prod_{n=k}^{i-1} \frac{a_{n+1,n}}{d_n} \left[\sum_{j=k}^{i-1} d_j \frac{e^{(-d_j t)} - e^{(-d_i t)}}{(d_i - d_j)} \prod_{\substack{n=k \\ n \neq j}}^{i-1} \frac{d_n}{d_n - d_j} \right] \quad \text{Eq. (10)}$$

by multiplication and division of $\prod_{n=k}^{i-1} d_n$. The first product in Eq.(10) has significance because it is the fraction of atoms of isotope k that follow a particular sequence of decays and captures. If this product becomes less than 10^{-6} , contributions from nuclide k and its precursors to the concentration of nuclide i are neglected. This procedure is unnecessary for evaluating the outer summation because all the terms in this sum are known to be positive. In order to avoid a division by zero when two removal constants are approximately equal ($d_i \approx d_j$), the second summation in Eq. (10) becomes:

$$\sum_{j=k}^{i-1} d_j t e^{(-d_j t)} \prod_{\substack{n=k \\ n \neq j}}^{i-1} \frac{d_n}{d_n - d_j} \quad \text{Eq.(11)}$$

An analogous expression is derived for the case when $d_n = d_j$. These forms of the Bateman equations are applied when two isotopes in a chain have the same diagonal elements or when a cyclic chain is encountered, in which case a nuclide is considered to be its own precursor. The new rate constant then can be thought of as the coefficient of $X_k(0)$, where the product over n is over the queue of short-lived nuclides. The exponential matrix method and the Bateman solutions complement each other in this approach. The exponential matrix method is quite accurate when the transition coefficients are small but has problems when including large rate constants; conversely the Bateman solution has some numerical difficulties for extremely small rate constants, but is stable and accurate for large rate constants. The point depletion algorithm as implemented in MPACT is summarized in Figure 1.

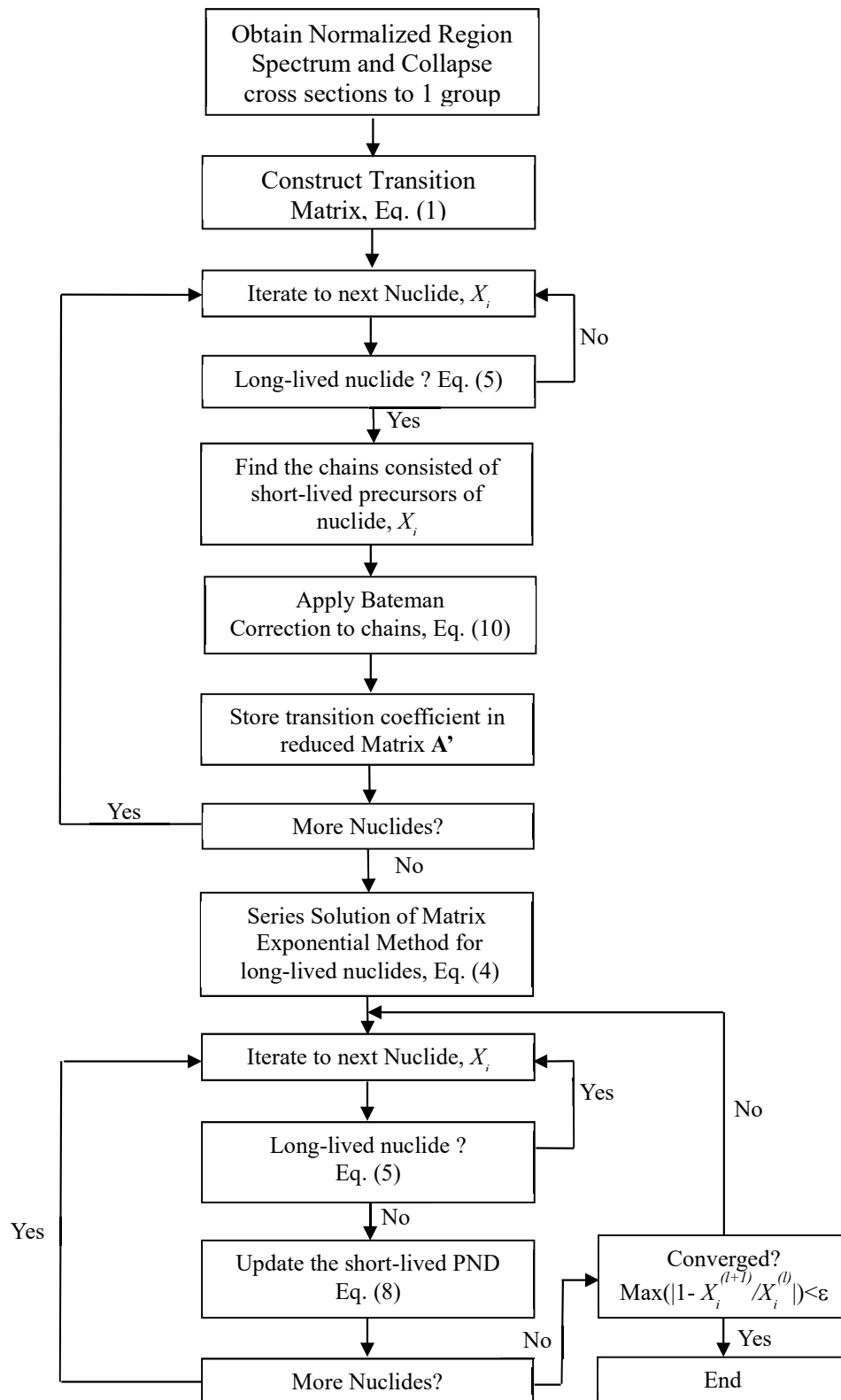


Figure 1: Point Depletion Algorithm

In MPACT, the flat flux regions of the fuel pin are azimuthally and radially dependent as shown on the left hand side of Figure 2. Currently, the depletable region of the pin is only radially dependent as shown on the right hand side of Figure 2. This has been shown to be adequate unless there are strong local asymmetries. The capability to treat azimuthally varying depletable regions is a simple modification, but will considerably increase memory requirements.

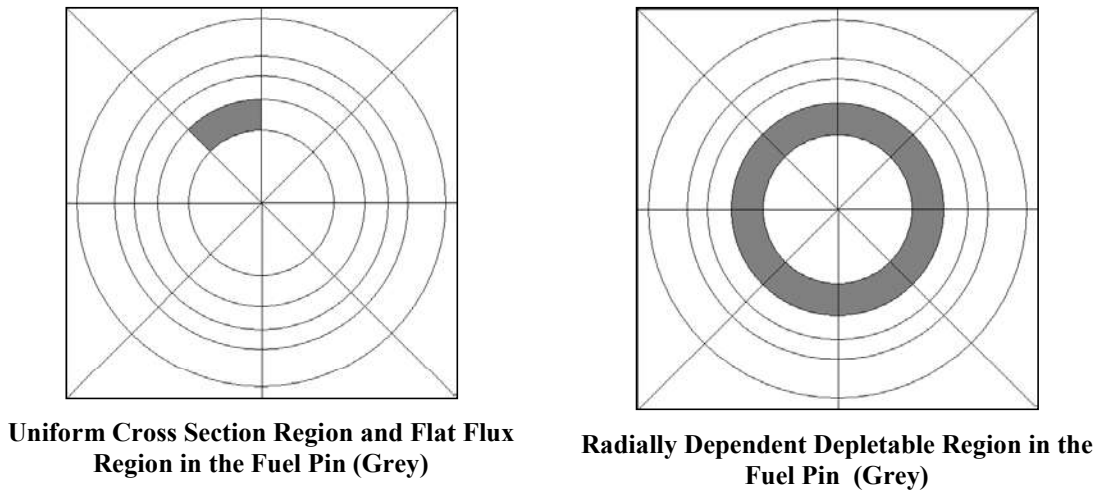


Figure 2: Depletion Zones in MPACT Pin Cell

In each step of a depletion calculation, the flux is assumed to be constant with time. There are several techniques for incorporating the time dependence of the flux into the depletion calculation. This is typically done by dividing the depletion problem into series of time steps, and periodically performing transport calculations. However, because the time dependence of the flux has non-linear feedback from the change in the fuel composition, the optimum depletion step size is often not known *a priori*, and to maintain an accurate solution the time steps are often very small leading to a longer computation time. Therefore, to reduce computation time and allow for longer burnup step sizes MPACT adopts two commonly used techniques: the predictor-corrector and sub-step methods. The predictor-corrector method works by computing a predicted nuclide concentration for a given time step, and then a corrected nuclide concentration. The basic predictor-corrector approach is:

$$N_{i2} = \frac{N_{i2}^P(\phi_{i1}, \sigma_{i1}) + N_{i2}^C(\phi_{i2}^P, \sigma_{i2}^P)}{2} \quad \text{Eq. (12)}$$

The predictor step includes the typical depletion calculation to obtain the particle number densities, $N_{i2}(\phi_{i1}, \sigma_{i1})$, at burnup t_2 by using the 1-group flux and cross section at the time of burnup t_1 . At this point the new predicted 1-group flux (ϕ_{i2}^P) and cross section (σ_{i2}^P) are obtained through a transport calculation using the predicted concentration, $N_{i2}^P(\phi_{i1}, \sigma_{i1})$. Next the corrector step performs a depletion calculation using the new 1-group flux (ϕ_{i2}^P) and cross section (σ_{i2}^P) and the new

corrected particle number densities, $N_{t_2}^C(\phi_{t_2}^P, \sigma_{t_2}^P)$, are obtained. The final particle number densities for t_2 are then taken to be the arithmetic mean of the predicted and corrected concentrations. Once N_{t_2} is obtained then a transport calculation is performed to obtain the steady state flux distribution at $t_2, (\phi_{t_2})$.

The sub-step method is applied to perform multiple depletion calculations between transport calculations. Since the depletion calculation typically takes less time than the transport calculation this will often save computational time. What this amounts to mathematically, is that the normalization factor, f , of the flux becomes time dependent but the eigenvector representing the flux distribution is still assumed to be constant between transport calculations. For M sub-steps the m^{th} flux, representing the flux at time $t_l + m\Delta t/M$, used by the depletion calculations is:

$$\phi_m = \phi_{t_l} f_{m-1}$$

$$\text{where } f_{m-1} = \frac{P_{t_l}}{\sum_j \sum_i N_{m-1}^{i,j} \kappa \sigma_{t_l}^{f,i,j} \phi_{t_l}^j} \quad \text{Eq. (13)}$$

where P_{t_l} is the total power at t_l , $\phi_{t_l}^j$ and $\kappa \sigma_{t_l}^{f,i,j}$ are the eigenvector for region j and the energy per fission multiplied by the microscopic fission cross section of region j and nuclide i at t_l , respectively, and $N_{m-1}^{i,j}$ is the nuclide concentration of $m-1$ sub-step. The sub-step method allows for even coarser burnup steps without a loss in accuracy. An overview of the depletion algorithm in MPACT is depicted in Figure 3.

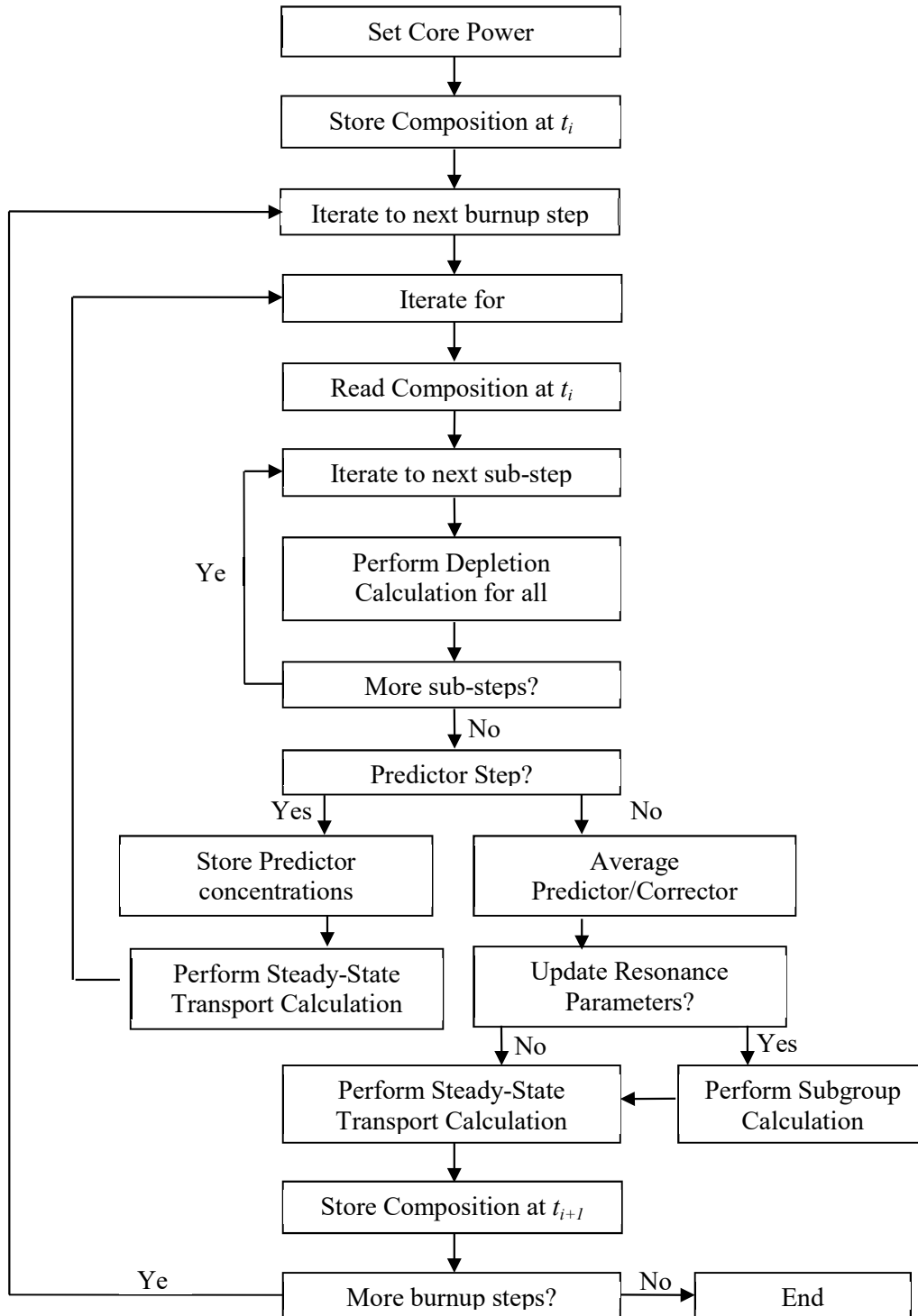


Figure 3: MPACT Depletion Algorithm

3.0 Boron 10 Depletion Methodology

The depletion of the boron 10 isotope is different from all of the other isotopes because the boron is dissolved into the coolant. Both isotopes of boron are present in the soluble boron but the B-10 isotope has a significantly higher neutron absorption cross-section. Without the addition of boron into the system (which is rare unless the power is significantly decreased), the B-10 concentration in the primary system can be modeled using a simple balance equation. The time rate change in the B-10 isotopes is equal to the difference in the sources and losses of B-10 isotopes:

$$\frac{dN_{B^{10}}(t)}{dt} V_{RCS} = -N_{B^{10}}(t) \sigma_{B^{10}} \int_{V_{core}} \phi dV$$

This equation can be solved for the number density of B-10 in the coolant as follows:

$$N_{B^{10}}(t) = N_{B^{10}}(0) e^{-\sigma_{B^{10}} \frac{\int_{V_{core}} \phi dV}{V_{RCS}} t}$$

$$\bar{\phi} V_{core} = \int_{V_{core}} \phi dV$$

$$\alpha_{core} = \frac{V_{core}}{V_{RCS}}$$

$$N_{B^{10}}(t) = N_{B^{10}}(0) e^{-\sigma_{B^{10}} \alpha_{core} \bar{\phi} t}$$

This equation can then be rewritten in terms of the atom fraction of B-10:

$$at\%_{B^{10}}(t) = \frac{N_{B^{10}}(t)}{N_{B^{10}}(t) + N_{B^{11}}}$$

$$at\%_{B^{10}}(t) = at\%_{B^{10}}(0) \frac{e^{-\sigma_{B^{10}} \alpha_{core} \bar{\phi} t}}{1 - at\%_{B^{10}}(0) (1 - e^{-\sigma_{B^{10}} \alpha_{core} \bar{\phi} t})}$$

This equation is used in MPACT to determine the B-10 atom fraction at every depletion step. The user has the ability to reset the B-10 concentration at any point in the cycle to simulate the addition of boron into the system or reset the B-10 fraction based on measurements.

4.0 Simplified Thermal Hydraulic Feedback

In previous work, CASL-U-2014-0051-000, MPACT was coupled to COBRA-TF to provide a detailed temperature and density distribution throughout the reactor core. Although this coupling was able to successfully provide an accurate distribution of power, temperature and density in the core, the computational complexity and cost was significant. There are several improvements that can be made to this coupling which are suggested in CASL-U-2014-0046-000 but most remain to be done as future work. In order to provide an initial solution for the AMA 9 benchmark, a simplified internal TH feedback model was implemented in MPACT.

The simplified TH model employs a 1D convection solution for each assembly and assumes every assembly in the core has an equal mass flow rate. The effects of pressure change are ignored and the equations are reduced to a simple energy balance for each axial node.

$$h_{out} = h_{in} + \frac{q}{\dot{m}}$$

The enthalpy is linearly interpolated to obtain the node average coolant enthalpy which is related to coolant temperature through a closure model.

Once the coolant temperature for each axial location is obtained, a 1D radial conduction model is used for every fuel pin with its specific power. The boundary condition for the fuel pin is set using a heat transfer coefficient and the modified Dittus-Bolter correlation proposed by Tong [1] is used to obtain the heat transfer coefficient.

$$q'' = h(T_s - T_{fluid})$$

$$Nu = \frac{hD_h}{k} = C Re^{0.8} Pr^{0.4}$$

$$C = 0.042 \frac{P_{pin}}{D} - 0.024$$

The conductivity through the cladding material is a 3rd order function of temperature and the gap conductance is fixed at 10,000 W/m²K. The fuel conductivity is unique for each cylindrical ring and is set to the following relationship on temperature.

$$k_{fuel} = 1.05 + \frac{2150}{T - 73.15} \frac{W}{mK}$$

The fuel temperature system is solved using a finite volume discretization of the fuel temperature assuming a uniform power density in the pin. The finite volume solver solves for the analytic temperature distribution inside an annular ring of with a constant thermal conductivity. The fuel is broken into several radial rings to capture the temperature effect on the thermal conductivity. Once the fuel temperature distribution is obtained, the volume average temperature is applied to MPACT.

All of the thermodynamic properties for the fluid were functionalized only to temperature (or enthalpy) using a quadratic fit for normal PWR operating conditions. Therefore the effects of pressure are neglected and all values are generated for 2250 psi. Since this simplified model is only used for scoping studies, these approximations will provide a reasonable feedback response with power. Further work will focus on obtaining the feedback from COBRA-TF.

5.0 Simulation of Watts Bar Cycle 1 Depletion

The demonstration of the full core depletion capability in MPACT was completed by approximating the first cycle of Watts Bar Nuclear Power Plant. The first approximation was to assume that the cycle is depleted at 100% power the entire operating cycle even though there was extended period of operational less than full power as shown in Figure 4 which shows the actual power history of Watts Bar through the entirety of cycle 1.

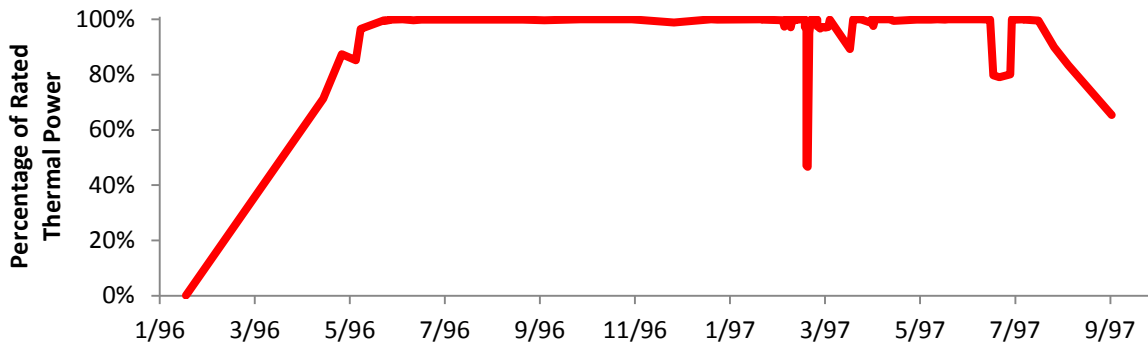


Figure 4: Watts Bar Cycle 1 Power History

The extended startup for the first cycle is not uncommon; however, it could potentially be a source of error by assuming the power is constant throughout the cycle. The small outage in the middle of the cycle would likely not have a significant effect on modeling the reactor depletion but the coast down at the end of the cycle will also affect the cycle length. This simulation was only run to 400 Effective Full Power Days (EFPD) which is just before the power coast down begins.

The second approximation in this simulation was to neglect the effects of equilibrium Xenon and Boron-10 depletion. Although both capabilities are in the code, the decision was made to leave both options off for the initial demonstration. The effects of equilibrium Xenon only affects the beginning of cycle when the power level in the pins is changing quickly. Since smaller time steps are used at the beginning of the cycle, this effect is likely small. The effects of Boron-10 depletion can become significant when the power is held constant for a prolonged period of time. The rate of depletion of boron-10 is about 0.005 at%/EFPD. Once the reactor is at full power in May 1996, the power is close to constant for 230 EFPD (Feb 1997). This will account for an approximate 1.15% decrease in B-10 atom percent from 19.9% to approximately 18.75% which would account for a 6% under-prediction of the boron concentration. This was not the effect observed and further studies will be performed to analyze this effect.

The demonstration case is run with the following time steps: 0, 10, 20, 30, 45, 60, 80, 100, 120, 160, 200, 240, 280, 320, 360, and 400 EFPD. The simulation was performed on the EOS computing cluster on 2088 cores. The simulation took 22 hours and 9 minutes to complete. The critical boron concentration was computed at every depletion step and is compared to the measured boron concentration in Figure 5.

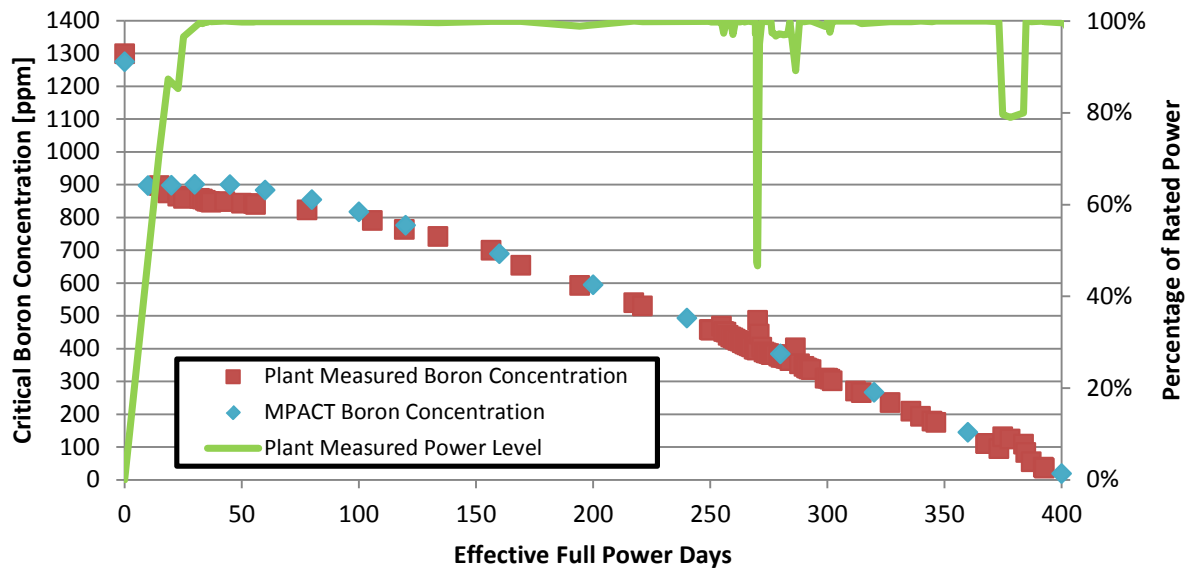


Figure 5: Watts Bar Cycle 1 Boron Letdown Curve

As indicated the data agrees very well with the measurement throughout the majority of the burnup cycle. The largest deviations from the measured boron concentration occur in the first 100 EFPD of operation. These deviations could be potentially caused by the approximations made during the initial power ramp as well as the lack of equilibrium Xenon modeling at the beginning of cycle. Another potential source of error is the scattering treatment. This simulation used P_0 scattering to reduce the computational requirements for this initial analysis, but it has been shown that significant power tilts can occur with P_0 is used. The scattering treatment will have the most significant effect at the beginning of life when larger power gradients occur. Later on in the cycle, the power shape becomes very flat, and the effect of the scattering treatment is considerably reduced. As noted before, a 6% over prediction around 260 EFPD (Feb 1997) was expected because of B-10 depletion, however, this effect is not seen in the simulation results. Further investigation is being made to understand this behavior.

In addition to calculating the critical boron concentration, MPACT edits the power at every point in the cycle. Figure 6 shows the predicted power distribution in Watts Bar at beginning, middle, and end of cycle. It can be observed that the larger pin power peaking observed at the beginning of the cycle is flattened and the power distribution in the core becomes more uniform at the end of cycle.

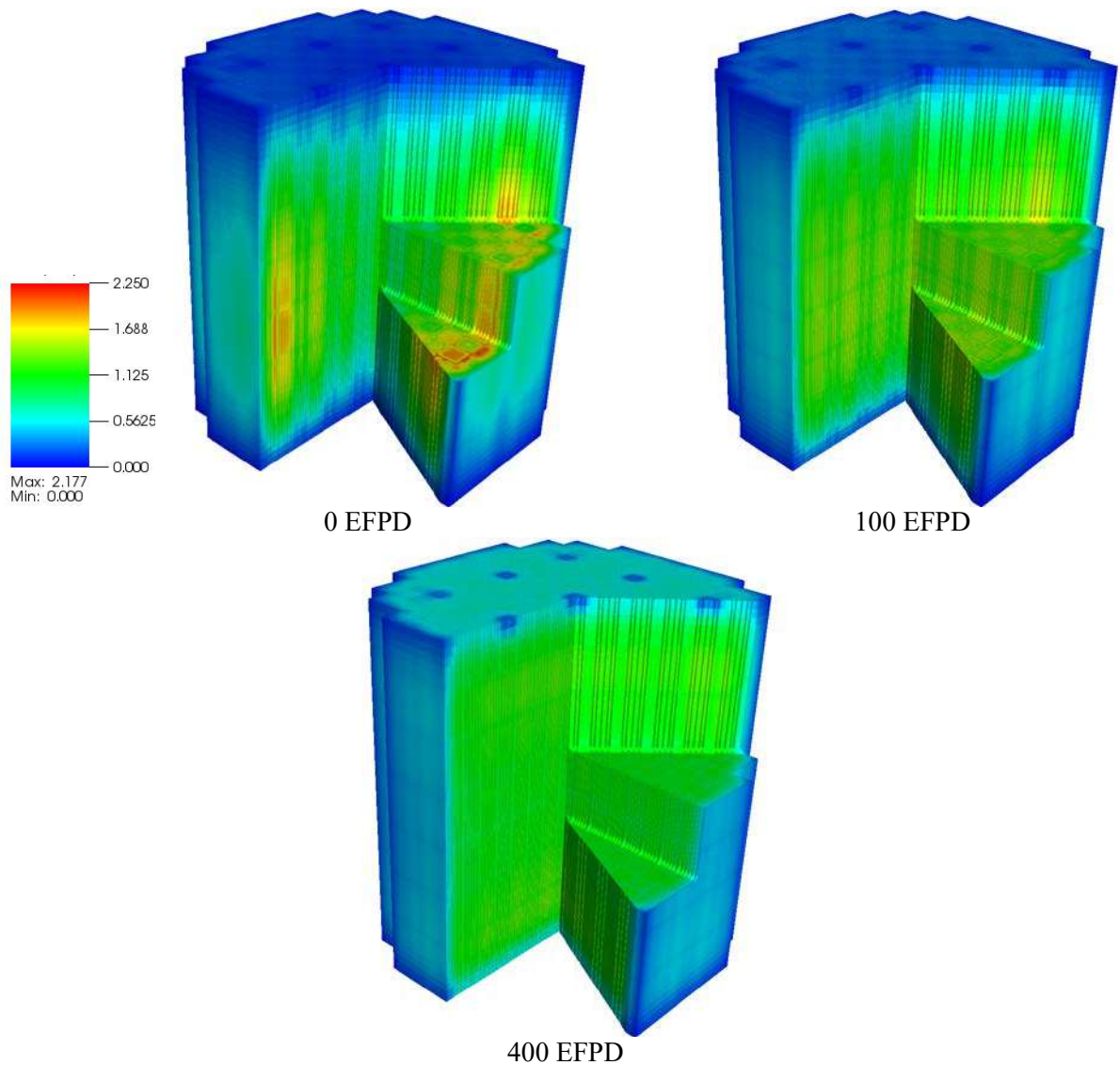


Figure 6: Pin Power Distribution during Depletion

6.0 Summary and Future Work

The objective of the milestone reported here was to develop and demonstrate the capability of MPACT to perform a 3D depletion for an operating cycle of a nuclear reactor. Several additional functionalities were added to MPACT in order to perform this calculation. These included the time dependent treatment of all isotopes in the reactor, a specialized treatment of the B-10 depletion effect, and the implementation of a simplified TH feedback model. The initial comparison with the measured data shows reasonably good results although a few approximations were made in the simulation which likely affected the accuracy. Future work will address each of these approximations:

- More accurate modeling of the reactor startup to demonstrate its effect on the core reactivity
- Accurate modeling of the treatment of Xenon at the beginning of the cycle
- Modeling of the depletion of B-10 during the simulation of the reactor. Since the data on boron additions isn't available, approximations will need to be made to determine how the B-10 concentration is reset after an extended power change

- Better treatment of anisotropic scattering which could either include a stable transport corrected P_0 scattering treatment or a higher order P_n scattering treatment
- Better treatment of the thermal hydraulic conditions in the reactor using Cobra-TF

Other improvements are also suggested to make the code more practical for full core reactor depletion calculations:

- Reducing the memory footprint.
The primary reason for running the calculation with P_0 scattering was the increased memory burden when tracking 510 isotopes throughout the entire core. Decreasing the memory burden would allow for better scattering treatment.
- Reducing the runtime of the problem.
This simulation required approximately 1 day to run on about 2000 cores but if P_n scattering is needed, the runtime requirements of this simulation could increase by a factor of 2-3. Areas for improvement in the runtime include; improved acceleration of the solution through CMFD, improved subgroup implementation, tighter coupling between 3D CMFD solver and 1D axial solvers, tighter coupling between CMFD and thermal hydraulics.
- Modeling the problem with more accurate thermal hydraulics
The original intent of this simulation was to use the Cobra-TF coupling that was developed in CASL-U-2014-0051-000 however it was determined that the large computational burden would have compromised the ability to complete this this milestone on time. The simplified TH model demonstrated a new coupling scheme that is much more efficient and reduced the total number of iterations. Implementing the new coupling scheme with the Cobra-TF code will increase the accuracy of the TH and yet provide an efficient computational scheme.

The other difficulty in completing this simulation was the availability of resources. When making requests for 1 day of wall time on 2000 cores, it would usually result in a queue wait time between 1 and 2 days. This means the entire simulation from submission to result took 2-3 days. Securing a more dedicated resource for these long computations would assist in the development, debugging, and assessment of these large problems and assist in the timely completion of milestones

References

1. Tong, L. S. and Weisman, J. (1979) *Thermal Analysis of Pressurized Water Reactors*, 2nd edn., American Nuclear Society, La Grange Park, Illinois.